PHYSICAL REVIEW B VOLUME 37, NUMBER 14 15 MAY 1988-I

Stark effect in strongly coupled quantum wells

S. R. Andrews, C. M. Murray, R. A. Davies, and T. M. Kerr
GEC Research Limited, Hirst Research Centre, East Lane, Wembley, Middlesex, HA9 7PP, United Kingdom
(Received 30 November 1987)

The energies and oscillator strengths of the excitonic transitions in a pair of strongly coupled quantum wells in the $GaAs/Al_xGa_{1-x}As$ system have been experimentally investigated as a function of electric field and compared with an effective-mass calculation which neglects band mixing. Good agreement with experiment can be obtained by taking into account nonparabolicity in the light-hole bands. Although not readily evident in the field dependence of the excitonic transition energies, band mixing has a measurable effect on exciton linewidths. The optoelectronic device implications of the Stark effect observed in this system are briefly considered.

I. INTRODUCTION

The optical properties of semiconductors fabricated in layers which are thin on the scale of the three-dimensional free-exciton diameter are strongly modified relative to those in the bulk crystals. In particular, in type-I semiconductor quantum wells, strong spatial confinement of both electrons and holes changes the parabolic energy dependence of the continuum absorption spectrum appropriate to three dimensions into a series of steps, and increases the exciton binding energies and oscillator strengths so that the excitonic features in the absorption spectrum can be clearly resolved, even at room temperature. One of the most dramatic effects of exciton confinement, and one which has attracted much recent interest, concerns the application of electric fields perpendicular to the layers. The lowest-energy excitonic absorption edge can be red shifted by energies greatly in excess of the binding energy while still remaining well-resolved, an effect which is unknown in the bulk, where the Stark shift of the 1*s* exciton is limited to a mere 10% of its binding energy before the resonance becomes severely broadened by field ionization. The origin of the persistence of exciton resonances to larger electric fields in a quantum well lies in the fact that tunneling of the electron and hole out of the exciton potential also necessitates tunneling out of the confining conduction- and valence-band potentials of the heterojunctions. A larger polarization of the exciton is therefore possible before ionization compared with the bulk semiconductor. This quantum-confined Stark effect[1,2] finds application in a variety of interesting electrooptic devices such as modulators[3,4] and bistable optical switches.[5,6]

Until recently, studies of the Stark effect in multiple-quantum-well structures have focused on the simplest case of square wells electronically isolated from each other by thick barriers. For example, in electroabsorptive device applications in $GaAs/Al_xGa_{1-x}As$ the optimum structure has a well width of about 10 nm, barrier widths in excess of 5 nm and an aluminum concentration in the barriers of about 30%.[7] The question naturally arises as to whether engineering of well or barrier shape and interwell coupling with the atomic-scale precision afforded by molecular-beam epitaxy can yield qualitatively different behavior and also possibly enhance certain electrooptic device functions. More complicated structures have indeed been fabricated but not usually with electrooptic properties directly in mind. For example, grading of the aluminum composition has been used to produce parabolic,[8] half-parabolic,[9] and double-step[9,10] quantum wells. The exciton transitions in these structures in zero external electric field have been investigated using photoluminescence excitation spectroscopy. Pairs of nominally identical quantum wells strongly coupled via a thin barrier have also been studied.[11-13] More recently, room-temperature electroabsorption in a strongly coupled quantum-well waveguide structure[14] and low-temperature luminescence excitation spectroscopy in an asymmetric coupled-well system[15] have been reported. In this paper we investigate in detail the effect of a static perpendicular electric field on the low-temperature exciton transition energies and oscillator strengths of a symmetrical pair of strongly coupled quantum wells and briefly consider the implications of the engineering of well coupling for quantum electrooptic devices.

II. EXPERIMENTAL DETAILS

The sample under study was grown by molecular-beam epitaxy to the following nominal specification: Si-doped GaAs(100) substrate, a 0.5-μm Si-doped GaAs buffer layer (10^{18} cm^{-3}), then layers of 20 nm $Al_{0.3}Ga_{0.7}As$, 20 nm GaAs, 40 nm $Al_{0.3}Ga_{0.7}As$, 5 nm GaAs, 1.4 nm $Al_{0.3}Ga_{0.7}As$, 5 nm GaAs, and 40 nm $Al_{0.3}Ga_{0.7}As$. The top seven layers were not intentionally doped. The structure is shown in the inset of Fig. 1 with slightly different values of well and barrier width as determined by fits to the theory described below. An electric field was applied perpendicular to the undoped GaAs quantum wells in a Schottky-barrier configuration formed by sputtering a 100-nm-thick, 3-mm-diameter transparent indium tin oxide (ITO) electrode onto the top surface.

Luminescence spectra at 5 K were excited with 0.1–1 W cm^{-2} of light from an argon-ion-pumped pyridine-2 dye laser, incident at 20° to the surface normal and polarized in the plane of the layers and with a line width of

 ©1988 The American Physical Society

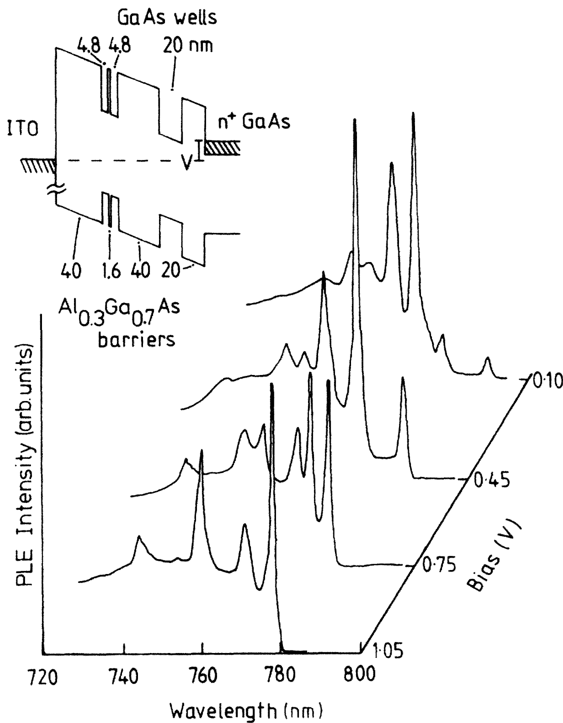

FIG. 1. Photoluminescence excitation spectra of the coupled quantum-well structure shown in the inset at various applied biases. The intensities in the spectra are scaled to agree at 730 nm.

about 0.05 meV FWHM (full width at half maximum). Light was collected at 90° to the incident beam and spectrally dispersed by a 0.85-m double-grating monochromator (resolution 0.1 meV) prior to detection using a cooled GaAs photomultiplier and photon counting.

III. RESULTS

Typical luminescence excitation spectra at different values of reverse bias are shown in Fig. 1. The spectrometer was set to detect near the center of the strong luminescence peak arising from recombination of the $n=1$ electron–$n=1$ heavy hole ($e1$-$h1$) "free" exciton. This emission was Stokes shifted by about 2 meV from the center of the $e1$-$h1$ absorption presumably because of binding to potential fluctuation arising from variations in well width. A small portion of each spectrum (essentially elastically scattered light), corresponding to the band pass of the spectrometer at the detection wavelength, has been removed from Fig. 1 for clarity. The spectra in Fig. 1 are scaled so that the intensity at 730 nm, well above the absorption edge, is independent of field. This scaling procedure is suggested by oscillator-strength sum rules discussed by Miller *et al.*[16] (their sum rule 3) and is appropriate in the approximation that the photoluminescence intensity is proportional to absorption. As a check on this the integrated intensity in the scaled spectra (from 730 nm to the $e1$-$h1$ excitonic band edge) was measured and found to be independent of the magnitude of reverse bias to within ±6% over the whole range investigated. This finding is in accord with a more rigorous sum rule (number 1) also discussed by Miller *et al.*[16] and gives us confidence in both our scaling procedure and our initial assumption of proportionality of luminescence intensity to absorption in the excitation spectra.

Zero electric field (i.e., flat band) in Fig. 1 corresponds to a bias of 1.05 V. This was inferred by assuming zero field to be that at which both the oscillator strength and energy of the $e1$-$h1$ transition are a maximum. This amounts to assuming that the structure is symmetrical, with both wells of equal width. The bias measured in this way is close to the saturation photovoltage obtained with excitation above the $Al_xGa_{1-x}As$ band gap.

At zero electric field the spectrum differs markedly from that of an isolated (barrier width $\gtrsim 10$ nm) 5-nm-wide quantum well which has only one bound conduction-band state with an aluminum mole fraction $x=0.30$ in the barriers and shows only two symmetry-allowed transitions ($e1$-$h1$ and $e1$-$l1$). The strong resonant coupling between the two wells in our sample splits each electron and hole state into symmetric (bonding) and antisymmetric (antibonding) states with the result that the spectrum qualitatively (but not quantitatively) resembles that expected for the 10-nm single quantum well obtained by removing the dividing barrier. The spectrum at zero field shows the symmetry-allowed $e1$-$h1$, $e1$-$l1$, $e2$-$h2$, and $e2$-$l2$ transitions and also a small peak at about 1.645 eV (753.5 nm) which we assign to the $e2$-$l1$ transition. This transition is symmetry forbidden in the absence of band mixing but can acquire some spectral weight when hybridization with the $h2$ states of the $e2$-$h2$ continuum is taken into account.[17] A small electric field or asymmetry in the structure could also contribute to the strength of this transition.

Application of a perpendicular electric field has two major effects on the exciton structure in the luminescence excitation spectrum. Firstly, it breaks the symmetry of the bound states with the result that additional "forbidden" exciton transitions appear in the spectrum (Fig. 1). The total oscillator strength, summed over all transitions, is conserved and consequently the forbidden transitions increase in intensity at the expense of those transitions which are symmetry allowed in zero field. Secondly, the exciton energies undergo interesting Stark shifts as shown in Fig. 2. The electric field scale in Fig. 2 is estimated by dividing the difference between the applied and built-in biases by the thickness of the undoped layers in the structure (confirmed by transmission electron microscopy). The assignment of the peaks in the excitation spectra to transitions between particular conduction- and valence-band states is based on calculations described below.

The variation of the exciton transition energies with field shown in Fig. 2 is qualitatively different from that expected from the isolated 5- or 10-nm-wide quantum wells to which the coupled-well system approximates in the limit of infinite and zero dividing barrier height (or width), respectively. In the single-well case the conduction- and valence-band states both shift to lower energy, but in such a way that there is a net Stark shift to

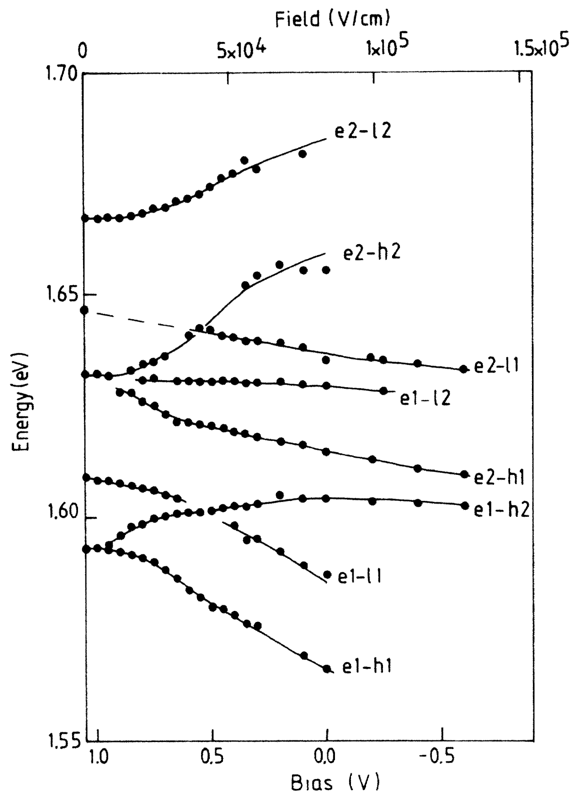

FIG. 2. Measured exciton peak energies as a function of bias obtained from spectra such as those in Fig. 1. The spectral assignments are based on the calculated curves shown in Fig. 3.

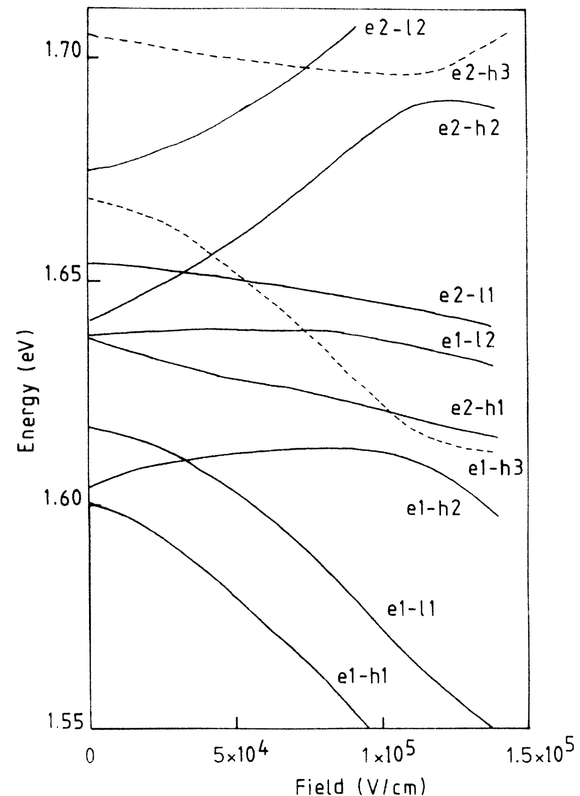

FIG. 3. Calculated transition energies (excluding exciton effects) for the coupled quantum well as a function of electric field. All transitions except those shown by dashed lines are clearly observed experimentally.

lower energy in the exciton transitions. This Stark shift is larger in the 10-nm well than in the 5-nm well, where strong spatial confinement prevents as large a charge polarization. In the coupled-well case the symmetric and antisymmetric states become hybridized in an electric field, leading to level repulsion and three different kinds of exciton transitions. Firstly, there are those which connect "symmetric" states which move together with increasing field ($e1$-$h1$ and $e1$-$l1$). These transitions undergo very large Stark shifts to lower energy (larger than in the 10-nm well case). Secondly, there are transitions connecting "antisymmetric" states which move apart with increasing field and undergo large Stark shifts to higher energy ($e2$-$h2$, $e2$-$l2$). Thirdly, there are transitions between symmetric and antisymmetric states (i.e., transitions which are forbidden in zero field) which move in the same direction with increasing field and show relatively small Stark shifts.

Figure 3 shows the transition energies in the coupled well (shown in the inset of Fig. 1) calculated neglecting the electron-hole Coulomb interaction. The single-particle eigenstates and energies were determined using the tunneling resonance method.[2] This is essentially a transfer matrix method in which it is assumed that changes in composition produce only an abrupt perturbation of the atomic potential and that there is continuity of the particle flux and carrier envelope wave functions at each interface. In the calculations we initially took the perpendicular effective masses in the GaAs quantum wells to be $m_e^{\perp}=0.067m_0$, $m_{\rm hh}^{\perp}=0.34m_0$, and $m_{\rm lh}^{\perp}=0.094m_0$ with a 57:43 band-offset ratio. These are the values arrived at by Miller and Kleinman[18] who fitted the same type of model to the measured transition energies in a series of wells, mostly with widths greater than about 10 nm. To obtain the best fit to the measured heavy-hole transition energies at zero field (assuming an average heavy hole exciton binding energy of 8 meV) we varied the well and barrier widths and aluminum composition about their nominal values. The optimized well and barrier widths were found to be 4.8 ± 0.1 nm and 1.6 ± 0.1 nm with an aluminum concentration in the barriers of 30 ± 2 %. However, using these parameters, we found that the light-hole transitions could only be fitted by using a larger perpendicular light-hole mass of $(0.125\pm0.010)m_0$. We attribute this to the effect of nonparabolicity in the light-hole band and discuss it further below.

Considering the approximations made, the calculation provides a surprisingly good description of the data in Fig. 2 and differs mainly in predicting larger Stark shifts for the transitions. This discrepancy probably arises from an inadequate estimation of the electric field, which is based on the assumption that voltage is dropped uniformly across the undoped thickness of the sample. The good agreement between calculation and experiment near the "crossing" of the $e1$-$l1$ and $e1$-$h2$ transitions shows

that band mixing, which is neglected in our calculations and in principle leads to level repulsion and anticrossing, has a fairly small effect on the transition energies. In a 5- or 10-nm $GaAs/Al_xGa_{1-x}As$ single quantum well such an anticrossing does not take place in an electric field, but can be obtained under uniaxial stress (at zero electric field) where similar behavior is observed.[19]

The effects of band mixing are more evident when the relative linewidths of the $e1$-$h1$ and $e1$-$l1$ transitions are compared (Fig. 4). The $e1$-$l1$ exciton is degenerate with the $e1$-$h1$ and $e1$-$h2$ continua at zero field. Mixing of the $l1$ with the $h1$ and $h2$ states gives rise to an additional homogeneous broadening of the $e1$-$l1$ Fano-like exciton resonance. Higher-lying transitions are similarly affected. The $e1$-$l1$ linewidth is 5.2 meV (FWHM) at zero field compared with 2.7 meV (dominantly inhomogeneous) for the $e1$-$h1$ exciton. The inhomogeneous broadening should be similar for heavy- and light-hole excitons and is probably dominated by fluctuations in well width of order ± 0.1 nm over distances larger than the exciton diameter. The inhomogeneous linewidth in our sample is calculated to be only 0.4 times as sensitive to fluctuations in the barrier width as to fluctuations in well width.

With increasing applied field the $e1$-$l1$ linewidth falls to a value similar to that of the $e1$-$h1$ transition. We attribute this reduction in linewidth to two factors. Firstly, at a field of about 4×10^4 V cm^{-1} the $e1$-$l1$ and $e1$-$h2$ transitions effectively cross so that for larger fields the discrete $e1$-$l1$ state is no longer degenerate with the $e1$-$h2$ continuum. Secondly, the $e1$-$h1$ and $e1$-$l1$ oscillator strengths are reduced with increasing field (as discussed below) but the former more rapidly so than the latter. This then leads to a reduced interaction between the $e1$-$l1$ discrete and $e1$-$h1$ continuum states. The slow increase in the $e1$-$h1$ exciton linewidth with field, evident in Fig. 4, can probably be attributed to the increased sensitivity of the wave functions to interface disorder at higher fields.[20]

To investigate the perpendicular light-hole mass further, experiments were also performed on a second sample which differed only in having 3.8-nm wells and 1.4-nm barriers. To fit the data in this case it was necessary to use a light-hole mass of $0.15m_0$. We mention this data, which was qualitatively similar in every respect to that of the first sample, only to emphasize the large perpendicular light-hole mass required to fit the data in both samples and will not discuss it further. Watanabe and Kawai[21] have used similar large light-hole masses to fit variable-temperature photoluminescence data[13] obtained from 3-nm wells coupled by $x=0.50$ barriers with widths between 1 and 2 nm. Both sets of results suggest that nonparabolicity in the light-hole bands (i.e., energy dependence of the effective mass) is important for confinement energies greater than about 50 meV. In our analysis, we have assumed that the light-hole nonparabolicity dominates and that we can neglect explicitly the smaller nonparabolicity in the electron and heavy-hole bands. We have also used an average mass for the $l1$ and $l2$ bands. In bulk GaAs nonparabolicity becomes pronounced in the light-hole band (caused mainly by interaction with the split-off band) at roughly 50 meV and in the conduction band at about 100 meV.[22] The effects of zone folding along $\mathbf{k}_\perp$ in the quantum well case might reasonably be expected to exaggerate the tendency of the light-hole bands to become heavy-hole-like at higher energy.

We have also compared the measured field dependence of the oscillator strengths of the exciton transitions with the calculated electron-hole overlap integrals $\langle\phi_e\,|\,\phi_h\rangle$, as shown in Fig. 5. Here $|\,\phi_e\rangle$ and $|\,\phi_h\rangle$ are the z components of the electron and hole wave functions determined in the tunneling resonance calculations. The oscillator strengths are assumed to be proportional to the integrated areas (above the continuum background) in the scaled excitation spectra. Experiment and calculation for each transition are adjusted to agree at either low or high

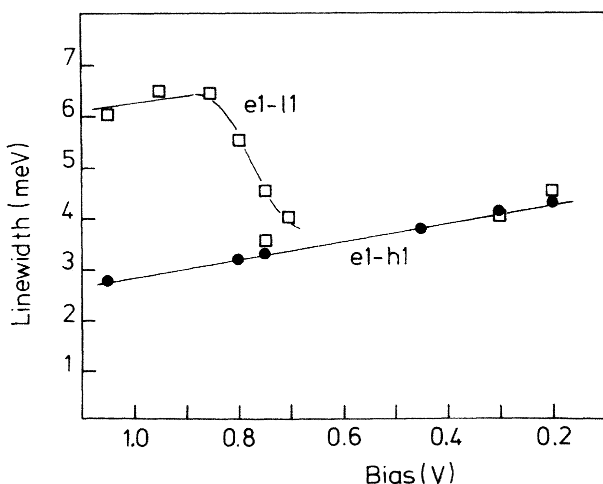

FIG. 4. Measured widths (FWHM) of the $e1$-$h1$ (circles) and $e1$-$l1$ (squares) transitions of the coupled quantum well as a function of the applied bias. Curves are guides to the eye.

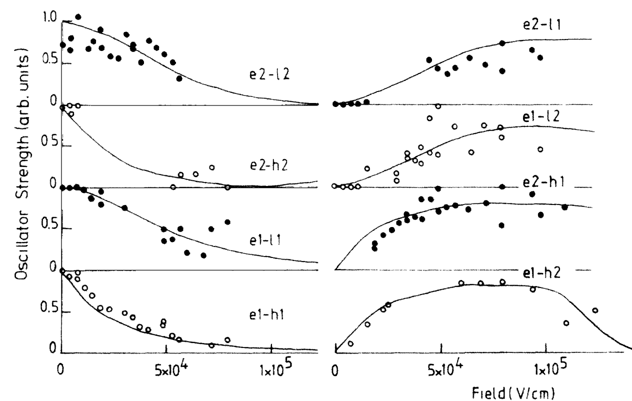

FIG. 5. Measured relative oscillator strengths of the coupled quantum-well exciton transitions as a function of the estimated applied electric field compared with the calculated square of the electron-hole overlap integrals (curves) normalized as described in the text.

field in Fig. 5. Estimation of the continuum background is not straightforward for many of the transitions, but there is reasonable qualitative agreement between calculation and experiment, confirming our assignments of the transitions in Figs. 2 and 5. It is not immediately obvious that the agreement should be expected to be good since the oscillator strengths also depend on the wave-function overlap in the plane of the wells (inversely as the square of the exciton Bohr radius). For example, the variational calculations described below show that there is an increase of 25% in the $e1$-$h1$ Bohr radius and therefore an additional 50% decrease in oscillator strength between 0 and 10^5 V cm^{-1}. However, another oscillator strength sum rule (Miller *et al.*[16] number 2) suggests that changes in other (possibly forbidden) transitions tend to compensate the measured intensity for this effect so that the comparison is probably reasonable.

The decrease in the $e1$-$h1$ oscillator strength with increasing field is particularly obvious in Fig. 1. The integrated luminescence intensity of the same transition was, however, approximately constant for biases between 0.2 and 1.1 V with excitation at 1.65 eV. This is presumably because the nonradiative recombination rate in this range of bias is small compared with the radiative recombination rate. Under these circumstances the integrated steady-state luminescence efficiency is independent of the radiative recombination rate[23] and therefore also of the $e1$-$h1$ oscillator strength. At large fields the integrated luminescence intensity decreases and the photocurrent increases as carriers begin to tunnel out of the wells before they can recombine.

The binding-energy calculations which we have referred to were performed variationally using a trial separable 1*s* exciton wave function of the form $\phi_e\phi_h \exp(-r/\lambda)$, where ϕ_e,ϕ_h are calculated by the tunneling resonance method and λ, the variational parameter, is the exciton diameter in the plane of the well. To describe the anisotropic dispersion in the valence bands near $\mathbf{k}=0$ we have used the diagonal form of the 4×4 Luttinger Hamiltonian[24] with incorporation of confinement in the *z* direction. This model neglects band warping and mixing. The perpendicular and parallel effective hole masses are given by

$$m_{hh}^{\perp}=m_0/(\gamma_1-2\gamma_2),\quad m_{hh}^{\parallel}=m_0/(\gamma_1+\gamma_2)\ ,$$

$$m_{lh}^{\perp}=m_0/(\gamma_1+2\gamma_2),\quad m_{lh}^{\parallel}=m_0/(\gamma_1-\gamma_2)\ .$$

We assume that the dielectric constant and Luttinger parameters γ_1,γ_2 are the same in $Al_xGa_{1-x}As$ as in GaAs. The results of the variational calculations for the $e1$-$h1$ and $e1$-$l1$ excitons in the coupled quantum well, for which we took $\gamma_1=5.47$ and $\gamma_2=1.26$ (corresponding to the larger light-hole mass), are shown in Fig. 6. For comparison we also show the variation in binding energies in a single 10-nm well obtained with $\gamma_1=6.79$ and $\gamma_2=1.92$. The latter Luttinger parameters correspond to the perpendicular masses preferred by Miller and Kleinman.[18] As expected, the $e1$-$h1$ binding energy in the coupled quantum well decreases more rapidly with field than in the single well, but still remains larger than the bulk binding energy at the highest fields investigated in our experiments. Using the same Luttinger parameters for both calculations does not affect the results qualitatively.

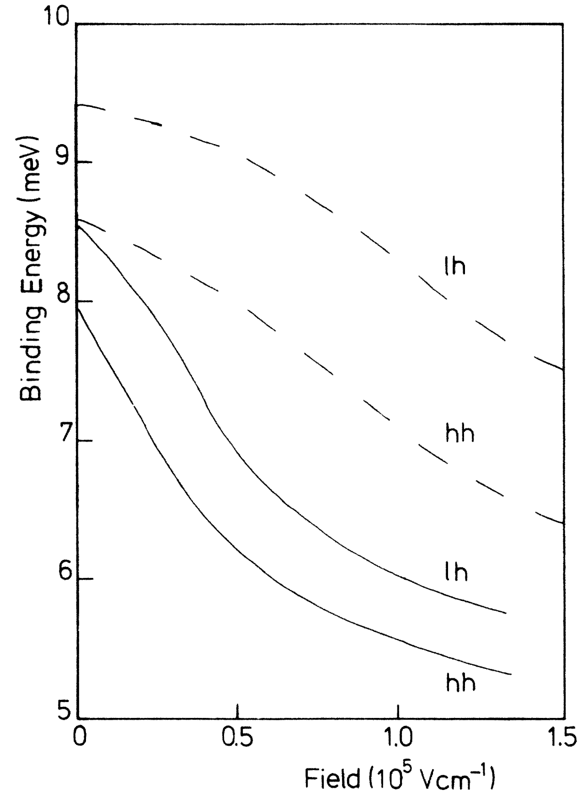

FIG. 6. Calculated binding energies of the $e1$-$h1$ and $e1$-$l1$ excitons (solid curves) in the coupled quantum well compared with those in an isolated 10-nm-wide square quantum well bounded by $Al_{0.3}Ga_{0.7}As$ barriers (dashed curves).

Our calculation underestimates the binding energies because of the neglect of the parallel effective mass discontinuity between GaAs and $Al_xGa_{1-x}As$,[25] and of the off-diagonal terms in the Luttinger Hamiltonian which mix light- and heavy-hole states away from $\mathbf{k}_{\parallel}=\mathbf{0}$. The latter hybridization gives rise to large in-plane hole subband nonparabolicity and can even produce negative zone-center hole effective masses. Interaction between the $l1$ and $h2$ states is particularly significant in the context of our binding-energy calculations because the energy separation of these states at $\mathbf{k}=0$ is reduced by application of an electric field (Figs. 2 and 3). In a 10-nm isolated square quantum well, the $e1$-$h1$ and $e1$-$l1$ exciton binding energies are underestimated by ~1 and ~2 meV, respectively, if band mixing effects are neglected.[26] In our case, inclusion of such coupling might possibly lead to a somewhat larger, field-dependent enhancement of the coupled-well binding energies shown in Fig. 6.

IV. SUMMARY AND CONCLUSIONS

In summary, we have investigated the dc Stark effect in a symmetrical pair of strongly coupled GaAs square quantum wells separated by a thin $Al_xGa_{1-x}As$ barrier.

A perpendicular electric field has a much more dramatic effect on the exciton transition energies and oscillator strengths in the strongly coupled quantum well than it has in the single isolated quantum well obtained by either removing the barrier between the wells or making it much thicker. Good agreement between an effective mass calculation and experiment is obtained simply by assuming a larger light-hole perpendicular effective mass than that appropriate to wider wells. This is direct evidence for nonparabolicity in the light-hole dispersion relations. Although reasonable agreement between the measured and calculated exciton transition energies can be obtained while neglecting valence-band mixing effects, hybridization of light- and heavy-hole states gives rise to large homogeneous broadening of the $e1$-$l1$ and higher-energy exciton transitions as evidenced by the electric field dependence of the $e1$-$l1$ linewidth.

Do strongly coupled quantum wells offer potential advantages over isolated square quantum wells in terms of their application to electroabsorption modulators? At first sight, there seems to be little or no advantage in using strongly coupled quantum wells in free-space propagation devices (i.e., where light propagates perpendicular to the layers) because the benefit of increased sensitivity of the energy of the $e1$-$h1$ transition to the field is counterbalanced by the concomitant reduction in oscillator strength with increasing field. The active optical path length in this geometry is generally limited by depletion effects and cannot be increased to compensate for the reduction in modulation depth with reduced oscillator strength. We have, however, only discussed strongly coupled wells. In weakly coupled systems, with thicker barriers, the electric field dependence of the dynamics of charge transfer between the wells may be sufficiently different as to lead to interesting new types of free-space propagation devices.[27]

In waveguiding geometries, on the other hand, strongly coupled quantum wells appear to have several advantages. Here, the loss in oscillator strength with increasing field can easily be compensated for by increasing the optical path length so that the larger (by a factor of up to 2 compared with a single 10-nm well) Stark shifts obtainable at moderate field might be exploited. For example, thin barriers are generally preferred in injection lasers so that monolithic integration of low-threshold-current lasers and efficient modulators[28] might be more easily achieved using strongly coupled quantum-well structures. Our calculations suggest that the reduction in binding energy with field is not so large as to present a problem for room-temperature operation.

Finally, introducing asymmetry into the structure by making the two well widths different has a qualitatively similar effect to applying an external field. This could allow the zero-bias operating point of a coupled quantum-well modulator on its Stark-shift–field curve to be engineered with some precision. This might be achieved in the single quantum-well case by grading the aluminum composition in the well,[29] but the problems in reproducibly fabricating graded structures on very small length scales are considerable.

Upon completion of this paper we learned of the recent experiments of Chen *et al.*[30] on a coupled system with 7.5-nm wells and 1.8-nm barriers. While our experimental observations are similar, we have made a more detailed comparison with theory which demonstrates that the behavior of the coupled-well system is well understood.

ACKNOWLEDGMENTS

This work was supported in part by the U.K. Joint Optoelectronics Research Scheme research programme. Some of the computations use techniques developed within the European Strategic Program for Research in Information Technology. We would like to thank W. M. Stobbs for the TEM verification of the layer thicknesses.

[1]D. A. B. Miller, D. S. Chemla, T. C. Damen, A. C. Gossard, W. Wiegmann, T. H. Wood, and C. A. Burrus, Phys. Rev. Lett. **53**, 2173 (1985).

[2]D. A. B. Miller, D. S. Chemla, T. C. Damen, A. C. Gossard, W. Wiegmann, T. H. Wood, and C. A. Burrus, Phys. Rev. B **32**, 1043 (1985).

[3]T. H. Wood, C. A. Burrus, D. A. B. Miller, D. S. Chemla, T. C. Damen, A. C. Gossard, and W. Wiegmann, Appl. Phys. Lett. **44**, 16 (1984).

[4]J. S. Weiner, D. A. B. Miller, D. S. Chemla, T. C. Damen, C. A. Burrus, T. H. Wood, A. C. Gossard, and W. Wiegmann, Appl. Phys. Lett. **47**, 1148 (1985).

[5]D. A. B. Miller, D. S. Chemla, T. C. Damen, A. C. Gossard, W. Wiegmann, T. H. Wood, and C. A. Burrus, Appl. Phys. Lett. **45**, 13 (1984).

[6]D. A. B. Miller, J. E. Henry, A. C. Gossard, and J. H. English, Appl. Phys. Lett. **49**, 821 (1986).

[7]D. S. Chemla, D. A. B. Miller, P. W. Smith, A. C. Gossard, and W. Wiegmann, IEEE J. Quantum Electron. **QE-20**, 265 (1984).

[8]R. C. Miller, A. C. Gossard, D. A. Kleinman, and O. Munteanu, Phys. Rev. B **29**, 3740 (1984).

[9]R. C. Miller, A. C. Gossard, and D. A. Kleinman, Phys. Rev. B **32**, 5443 (1985).

[10]M. H. Meynadier, C. Delalande, G. Bastard, M. Voos, F. Alexandre, and J. L. Lievin, Phys. Rev. B **31**, 5539 (1985).

[11]R. Dingle, A. C. Gossard, and W. Wiegmann, Phys. Rev. Lett. **34**, 1327 (1975).

[12]G. Bastard, U. O. Ziemelis, C. Delalande, M. Voos, A. C. Gossard, and W. Wiegmann, Solid State Commun. **49**, 671 (1984).

[13]H. Kawai, J. Kaneko, and N. Watanabe, J. Appl. Phys. **58**, 1263 (1985).

[14]M. N. Islam, R. L. Hillman, D. A. B. Miller, D. S. Chemla, A. C. Gossard, and J. H. English, Appl. Phys. Lett. **50**, 1098 (1987).

[15]H. Q. Le, J. J. Zayhowski, and W. D. Goodhue, Appl. Phys. Lett. **50**, 158 (1987).

[16]D. A. B. Miller, J. S. Weiner, and D. S. Chemla, IEEE J. Quantum Electron **QE-22**, 1816.

[17]G. D. Sanders, and Y. C. Chang, Phys. Rev. B **31**, 6892 (1985).
[18]R. C. Miller and D. A. Kleinman J. Lumin. **30**, 520 (1985).
[19]E. S. Koteles, C. Jagannath, J. Lee, Y. J. Chen, B. S. Elman, and J. Y. Chi, in *Proceedings of the 18th International Conference on the Physics of Semiconductors, Stockholm, 1986* edited by O. Engström (World-Scientific, Singapore, 1986), p. 625.
[20]S. Hong and J. Singh, Appl. Phys. Lett. **49**, 331 (1986).
[21]N. Watanabe and H. Kawai, J. Appl. Phys. **60**, 3696 (1986).
[22]J. S. Blakemore, J. Appl. Phys. **53**, R123 (1982).
[23]R. C. Miller, D. A. Kleinman, W. A. Nordland, and A. C. Gossard, Phys. Rev. B **22**, 863 (1980).
[24]J. M. Luttinger, Phys. Rev. **102**, 1030 (1956).
[25]C. Priester, G. Allan, and M. Lunnoo, Phys. Rev. B **30**, 7302 (1984).
[26]D. A. Broido and L. J. Sham, Phys. Rev. B **34**, 3917 (1986).
[27]J. W. Little, J. K. Whisnant, R. P. Leavitt, and R. A. Wilson, Appl. Phys. Lett. **51**, 1786 (1987).
[28]S. Tarucha, and H. Okamoto, Appl. Phys. Lett. **48**, 1 (1986).
[29]K. Nishi and T. Hiroshima, Appl. Phys. Lett. **51**, 320 (1987).
[30]Y. J. Chen, E. Koteles, B. S. Elman, and C. A. Armiento, Phys. Rev. B **36**, 4562 (1987).